Tau seeding in chronic traumatic encephalopathy parallels disease severity

Sarah K. Kaufman[1], **Sarah Svirsky**[2,3,4], **Jonathan D. Cherry**[2,5,6], **Ann C. McKee**[2,3,5,6,7], **Marc I. Diamond**[1]

[1]Center for Alzheimer's and Neurodegenerative Diseases, Peter O'Donnell Jr. Brain Institute, University of Texas Southwestern Medical Center, NL10.120, 6000 Harry Hines Blvd., Dallas, TX 75390, USA

[2]Alzheimer's Disease and Chronic Traumatic Encephalopathy Center, Boston University School of Medicine, Boston University, Boston, MA, USA

[3]Department of Neurology, Boston University School of Medicine, Boston, MA, USA

[4]Department of Neurological Surgery, University of Pittsburgh, Pittsburgh, PA, USA

[5]Department of Pathology and Laboratory Medicine, Boston University School of Medicine, Boston, MA, USA

[6]VA Boston Healthcare System, US Department of Veteran Affairs, Boston, MA, USA

[7]Edith Nourse Rogers Memorial VA Medical Center, Bedford, MA, USA

Abstract

Chronic traumatic encephalopathy (CTE), a neurodegenerative tauopathy, is associated with behavioral, mood and cognitive impairment, including dementia. Tauopathies are neurodegenerative diseases whose neuropathological phenotypes are characterized by distinct histopathologic features of tau pathology, which progressively deposit throughout the brain. In certain tauopathies, especially Alzheimer's disease (AD), tau deposition appears to follow brain network connections. Experimental evidence suggests that the progression of tau pathology in humans, mouse and cell models could be explained by tau seeds that adopt distinct conformations and serve as templates for their own amplification to mediate transcellular propagation of pathology. Tau seeds are efficiently detected by the induction of aggregation in cell-based "biosensors" that express tau repeat domain (RD) with a disease-associated mutation (P301S) fused to complementary fluorescent protein tags (cyan and yellow fluorescent protein). Biosensors enable quantification of tau seeding in fixed and fresh-frozen brain tissue. Phospho-tau deposition in CTE follows progressive stages (I–IV), but the relationship of seeding to this deposition is unclear. We have used an established biosensor assay to independently quantify tau seeding as compared to AT8 phospho-tau histopathology in thin sections of fixed tissues of 11 brain regions from 27 patients with CTE, 5 with other tauopathies, and 5 negative controls. In contrast to prior studies of AD, we detected tau seeding late in the course of CTE (predominantly stages III and IV). It was less anatomically prevalent than AT8-positive inclusions, which were relatively

✉Marc I. Diamond, marc.diamond@utsouthwestern.edu.

widespread. We especially observed seeding in the limbic system (amygdala, thalamus, basal ganglia), which may explain the dominant cognitive and behavior impairments that characterize CTE.

Introduction

Chronic brain trauma has long been recognized as a cause of dementia. In 1928, Harris Martland characterized "punch-drunk" syndrome in boxers by confusion, impaired balance, and slowed movements that typically progressed to overt Parkinsonism with dementia [20]. Now termed chronic traumatic encephalopathy (CTE), this progressive syndrome has been linked to repetitive head trauma from a variety of sources, including contact sports [22, 23, 33], head-banging [12] and military activities [13].

CTE is defined neuropathologically by intraneuronal accumulation of the microtubule-associated protein tau, which is detected by anti-phospho-tau antibodies such as AT8 [21]. A NINDS-NIBIB consensus meeting of expert neuropathologists determined the specific tau histopathology observed in CTE is unique and distinctive from all other tauopathies [4, 21]. The cortical phospho-tau pathology of CTE is heterogeneous and consists of neurofibrillary tangles (NFTs), pretangles, dotlike and threadlike neurites, and astrocytic inclusions [3, 6, 21]. Perivascular CTE lesions are immunopositive for 3R and 4R tau. In early stages of disease (CTE I/II) 4R tau predominates, and phospho-tau is found primarily in neurons. Beginning at age 60 and rising in each subsequent decade, phospho-tau (4R) astrocytes progressively increase in CTE lesions [6]. Astrocytes in CTE contain exclusively 4R tau, and are found at CTE stages III and IV. Neurons in CTE accumulate 3R and 4R tau, although young brain donors with mild CTE (I/II) accumulate only 4R neuronal tau pathology. The proportion of 3R neuronal tau pathology increases with age [6].

Pathogenic progression of CTE pathology is categorized by four discrete stages. In Stage I, phospho-tau foci occur around small vessels within the sulci of the frontal and temporal cortices; there are usually phospho-tau neurofibrillary tangles (NFTs) in the locus coeruleus (LC) [1, 24]. In Stage II, 3 or more perivascular foci occur in the cortex, and phospho-tau NFT appear in entorhinal cortex, amygdala, substantia nigra (SN) and LC [24]. In Stage III, phospho-tau pathology is widespread with the NFT in the frontal and temporal lobes, entorhinal cortex, amygdala, CA1, CA2 and CA4 hippocampus, thalamus, SN and LC [1]. In Stage IV, tau pathology is widespread in the cerebral cortex (with the exception of the primary visual cortex) and the medial temporal lobe, diencephalon, brainstem and cerebellar dentate nucleus [24, 28]. This pattern of progressive regional phospho-tau pathology in CTE has been confirmed by semi-quantitative and quantitative assessment and cluster analysis of the semi-quantitative rating scales in 366 cases of CTE [1].

The molecular mechanisms that underlie CTE are unknown. Accumulation of phospho-tau places CTE within the larger family of neurodegenerative tauopathies, which includes Alzheimer's disease, progressive supranuclear palsy, and frontotemporal lobar degeneration, among many others [19]. Tauopathies feature degeneration of neural networks [5, 36]. Extensive experimental evidence suggests that transcellular propagation of tau assemblies, defined as tau "seeding," underlies their inexorable progression [35]. Previous morphometric

analysis of CTE tau pathology suggests the heterogeneity seen across CTE patients may be due to different sites of initial brain trauma and subsequent spread of tau aggregates along distinct anatomic pathways [3]. In human AD tissue and experimental AD mouse models, tau seeding appears in the brain before histopathology reveals phospho-tau accumulation [11, 14, 18]. Tau assemblies derived from CTE brain lysates serve as templates for recruitment of naïve tau monomer, and thus propagate distinct assembly conformations, or "strains", in cell and mouse models [16, 37]. CTE-derived tau assemblies have a distinct conformation compared to AD (NFTs) [9], and a CTE-derived tau strain induces distinct patterns of tau histopathology that propagate in culture and a mouse tauopathy model [16], akin to what is observed in prion diseases. In summary, propagation of tau seeds of specific conformation may underlie the progression pattern of CTE pathology.

To monitor tau seeding in human tissue samples, we previously developed a quantitative, sensitive and specific cellular bioassay that works for fresh-frozen [14] or fixed tissue samples [18]. This is based on the use of cell lines that stably express the tau repeat domain (RD) with the disease-associated P301S mutation fused to cyan and yellow fluorescent protein. Tau aggregation produces fluorescence resonance energy transfer (FRET) that is reliably quantified across a wide dynamic range by flow cytometry. Incorporation of the P301S mutation enhances the sensitivity of this cell line to femtomolar concentrations (monomer equivalent) of recombinant tau fibrils [14]. This assay was previously used to characterize tau seeding in fixed human AD and progressive age-related tauopathy (PART) tissue [18]. In this study, we have determined how post-mortem phospho-tau histopathological assessment of CTE diagnosis correlates with seeding across multiple brain regions and stages.

Methods

IRB review and informed consent

Next of kin provided written consent for participation and brain donation of each subject in this study. Institutional Review Board approval for brain donation was obtained through the Boston University School of Medicine and Edith Nourse Rogers Memorial VA Medical Center, Bedford, MA. IRB approval for postmortem clinical record review, interviews with family members, and neuropathological evaluation was obtained through Boston University School of Medicine.

Clinical evaluation

CTE subjects—Clinical data were obtained through online surveys and retrospective telephone clinical interviews with informants, as described previously, including head injury exposure and neurodegenerative disease history [2, 27, 28]. To be considered a professional football player, a participant must have played in at least 1 regular season NFL game. Additional demographic and clinical information was obtained through review of medical records, and informant-reported race was recorded. A neurologist and/or neuropsychologist with expertise in neurodegenerative disorders conducted telephone clinical interviews with informants to obtain medical and clinical histories, including the presence, nature, and timeline of symptoms associated with cognition, behavior or mood, and daily functioning.

A consensus diagnosis of dementia was adjudicated based on modified Diagnostic and Statistical Manual of Mental Disorders (Fourth Edition, Text Revision) criteria.

Controls, Alzheimer's disease (AD) and frontotemporal lobar degeneration (FTLD)-tau subjects—Controls, subjects with Alzheimer's disease (AD) and Frontotemporal Lobar Degeneration (FTLD)-tau were evaluated by the Clinical Core of the Boston University Alzheimer's Disease Research Center (BU ADRC). A diagnosis of Control or Dementia was made by a BU ADRC multidisciplinary diagnostic consensus panel, following presentation and discussion of all examination and test findings, neuropsychological test scores, functional measures, as well as social, family, and medical history. Established criteria were used to determine AD dementia [25, 26].

Neuropathological evaluation

Pathological processing and evaluation were conducted using previously published methods [27, 28]. Brain volume and macroscopic features were recorded. Twenty-two sections of paraffin-embedded tissue were stained for Luxol fast blue, hematoxylin and eosin, Bielschowsky silver, phosphorylated tau (ptau) (AT8), α-synuclein, amyloid-β, and phosphorylated transactive response DNA binding protein 43 kDa (pTDP-43) using methods described previously. In some cases, large coronal slabs of the cerebral hemispheres were also cut at 50 μm on a sledge microtome and stained as free-floating sections using AT8 or CP-13.

A neuropathological diagnosis was made using criteria for CTE [4, 21] and well-established criteria for other neuropathological diseases, including AD, Lewy body disease, FTLD, and motor neuron disease. Neuropathological criteria for CTE require at least 1 perivascular phospho-tau lesion consisting of phosphorylated tau aggregates in neurons, with or without astrocytes, around a small blood vessel; these pathognomonic CTE lesions are most often distributed at the depths of the sulci in the cerebral cortex and are distinct from the lesions of aging-related tau astrogliopathy. Neuropathological diagnosis of AD was based on National Institute on Aging-Alzheimer's Association guidelines [31].

Subject disease classification

Subjects for this study were chosen based on their neuropathological diagnosis of CTE, AD, FTLD or controls.

Human tissue fixation and immunohistochemistry

Human tissue was fixed in periodate–lysine–paraformaldehyde (PLP) and stored at 4 °C. Blocks were paraffin-embedded for sectioning. Serial 10 μm sections were cut for subsequent experiments: sections 1–3 were stored in absolute alcohol for tau seeding and section 4 was mounted for immunohistochemistry. Mounted sections were incubated overnight at 4 °C in primary antibody phosphorylated PHF-tau (AT8; Pierce Endogen, Rockford, IL; 1:2000), then treated with biotinylated secondary antibody and labeled with a 3-amino-9-ethylcarbazol HRP substrate kit (Vector Laboratories, Burlingame, CA). Sections were counterstained with Gill's hematoxylin (Vector Laboratories) and mounted

with Permount medium (Thermo Scientific, Rockford, IL). Slides were scanned at 20× magnification using a Leica Aperio Scanscope (Leica Biosystems, Richmond, IL).

Digital analysis of tau pathology

Analysis was conducted as previously described using Aperio ImageScope (Leica Biosystems) [7]. Briefly, whole sections were outlined to quantify the total AT8 + immunoreactivity and total number of phospho-tau-containing cells. Automated image analysis algorithms for each measure were created using Aperio default macros as a backbone. The Aperio-positive pixel algorithm v9 was utilized to determine the total amount of AT8 staining by counting the number of positively stained pixels. The algorithm was designed to capture the overall total density of all AT8 staining in a given area. The algorithm was optimized on negative and positive sections to distinguish background vs. immunopositive staining. The number of positively stained pixels was then standardized to the area measured and presented as "AT8 positive pixels/mm^2".

The number of cells that contained phospho-tau was counted using a modified version of the Aperio nuclear algorithm v9. Using the AT8 stain, the nuclear algorithm was trained to recognize aggregates of phospho-tau that were consistent with a neuronal morphology. Roundness, elongation, compactness, and size thresholds were all set to capture neurons that contained tau. Although the algorithm was optimized to identify phospho-tau positive neurons, due to variable cellular morphology, it is likely that some phospho-tau-positive astrocytes were also counted. The counts were standardized to the area measured and reported as "Tau + cell/mm^2".

Selection of tissue sections for seeding assay

Tissue blocks included the following brain regions: 1. midbrain at level of the red nucleus, 2. inferior parietal cortex, 3. anterior cingulate, 4. lateral frontal cortex, 5. Superior temporal cortex, 6. amygdala/EC, 7. globus pallidus/putamen with insula, 8. hippocampus with LGN, 9. thalamus/sub-thalamic nucleus, 10. Upper pons including the locus coeruleus, 11. cerebellum. These blocks were selected based on previous work that identified brain regions of interest in CTE [24], and are the majority of regions included in the consensus criteria recommendations for evaluation of CTE [21].

Extraction of tau seeding

Brain sections taken immediately adjacent to those used for histopathology were stored in 100% ethanol at 4 °C until preparation for the seeding assay. Excess paraffin was removed with heated 100% ethanol washes at 60 °C as described previously [17]. Samples were then placed into 100 μL of 1 × TBS with protease inhibitors (Sigma-Aldrich complete protease inhibitor, EDTA free), and water bath sonicated in PCR tubes at 50% power at 4 °C for 120 min (Qsonica Q700 power supply, 431MPX microplate horn, with chiller). Samples were then diluted to 100 mm^3 of total tissue per 1 mL of TBS with protease inhibitors (v/v).

Culture of biosensor cells

A previously published biosensor cell line expressing tau-RD(P301S)-CFP and tau-RD(P301S)-YFP (ATCC CRL-3275) was used to perform all seeding assays. HEK293 cells

were grown in Dulbecco's modified Eagle's medium (DMEM) (Gibco) with 10% fetal bovine serum (Sigma) and 1% penicillin/streptomycin (Gibco). Cells were cultured at 37 °C, 5% CO_2 in a humidified incubator.

Transduction of biosensor cell lines

Biosensor cells were plated in 96-well plates as previously described [10, 17], with 25,000 cells per plated per well. At 18 h, cells were transduced with human tissue samples using Lipofectamine 2000 (Thermo Fisher Scientific). Homogenized human tissue samples were added to Opti-MEM (Thermo Fisher Scientific) and incubated for 5 min (3.3 μL lysate with 6.7 μL of Opti-MEM per well). Lipofectamine 2000 was incubated with Opti-MEM (1.25 μL Lipofectamine to 8.75 μL Opti-MEM per well) for five minutes. Lipofectamine complexes were then mixed with samples and incubated for 20 min prior to addition in triplicate to cells.

Biosensor cell preparation

All samples were assessed in triplicate. Cells were kept at 37 °C in a humidified incubator for 60 h, and subsequently dissociated with trypsin and prepared for analysis by flow cytometry. Biosensor cell lines were harvested with 0.05% trypsin, and quenched with media (DMEM + 50% FBS, 1% Pen/Strep, 1% Glutamax). Cells were spun at $500 \times g$ and resuspended in 2% PFA in $1 \times$ PBS. Cells were subsequently spun and resuspended in flow buffer (HBSS + 1% FBS + 1 mM EDTA) and stored for less than 24 h prior to performing flow cytometry.

Flow cytometry FRET analysis of tau seeding

Flow cytometry for all samples was performed using a BD Biosciences LSR Fortessa. Flow cytometry data were analyzed as previously described [10]. Seeding was calculated as (percentage of FRET-positive cells) × (median fluorescence intensity), which was normalized to negative control samples.

Statistical analysis

Flow cytometry and analysis of seeding in each sample was performed in a blinded fashion. Thresholds were set based on signal 5SD above baseline, as published in previous work [18]. Statistical analysis and graphical representations were performed using GraphPad PRISM.

Results

Table 1 provides a summary of the demographics, neuropathological findings, dementia status, and cause of death of the brain donors. Seven subjects with CTE had modest numbers of diffuse plaques, none had neuritic plaques and none were diagnosed with AD. None of the CTE subjects had Lewy bodies. Two had vascular disease in the form of 3 or more remote cortical microinfarcts. Eight subjects with CTE were also diagnosed with limbic-predominant age-related TDP-43 encephalopathy (LATE) [32].

Tau histopathology

We provide examples of histopathology from CTE cases in Stages I–IV (Figs. 1 and 2). Mild CTE cases (CTE Stages I/II) were not readily scored by automated histopathologic analysis and were classified by semi-quantitative evaluation by a neuropathologist (A.C.M.). In Stages I/II, relatively small regions of positive phospho-tau pathology were observed primarily at the depths of sulci. In contrast, phospho-tau pathology was detected throughout the brain in many cases of CTE Stages III/IV. Because of low aggregate density, when quantified in an automated fashion as previously described [7], only a small number of samples in CTE Stages I/II displayed positive tau histopathology ("AT8 positive pixels/ mm^2") and tau-positive cells ("Tau + cell/mm^2") above control samples (Fig. 3a, b). We evaluated two cases of CTE Stage IV which had distributions of AT8 signal similar to Stage III (Fig. 3). Results are displayed on a linear scale using a 5 standard deviation (SD) cutoff for positive signal above the average of negative control samples.

Tau seeding assay

Tau seeding distributes over a range of assembly sizes, from monomer to multimer [29, 30]. To quantify this activity we have previously developed a cellular biosensor system in which cultured HEK293T cells express the amyloid forming tau RD containing a single disease-associated mutation (P301S) fused to cyan and yellow fluorescent proteins (tau RD(P301S)CFP/YFP) [10, 14]. This cell line is freely available (ATCC CRL-3275). Identical or similarly constructed biosensors have been used by multiple laboratories to quantify tau seeding [8, 37]. The cells function by reacting to pathogenic tau conformers, which, for maximal sensitivity, are transduced using a cationic lipid (Lipofectamine 2000). This initiates intracellular aggregation of tau with very high specificity [14, 34], which is detected with flow cytometry by counting many thousands of individual cells within a 96- or 384-well plate. The assay is sensitive to seeds into the femtomolar range of tau monomer equivalent, and has a linear range over several log orders both for tau input and signal output [14]. Importantly, the assay detects seeds in both fresh-frozen [11] and formalin-fixed tissues [17, 18]. We have previously used this method to classify brains from AD cases, revealing seeding that anticipates AT8 positive signal across multiple brain regions [11, 18].

We ensured blinded evaluation of CTE cases at all times during tissue processing and analysis. The decode list was used only after all samples had been analyzed by flow cytometry. Samples were first processed with warm EtOH washes to solubilize and remove paraffin. Samples were then homogenized in a water bath sonicator. Since it is not feasible to use standard chemical assays to measure total protein in formalin-fixed samples, we standardized our analyses against total tissue volume per TBS volume. Biosensor cells were plated in 96-well format and exposed in triplicate to 3.3 μL of homogenized lysate per well, complexed with Lipofectamine 2000. Cells were incubated for 60 h prior to fixation and analysis on flow cytometry.

Tau seeding in CTE

We scored the seeding on a normalized logarithmic scale. To reduce false-positive samples, the threshold for tau seeding activity was set at 5 SD above the mean signal derived from several control samples without evident tauopathy (based on the absence of AT8 staining on

histopathologic analysis), as described previously [18]. We observed no appreciable seeding in any CTE brain region at stage I/II (Fig. 4). This indicates either that seeding in these samples is below the threshold of detection in the biosensor system, or that the AT8-positive signal observed in sparsely populated neurons does not represent seeding pathology. Seeding was strong across multiple regions at stages III/IV. Seeding was most consistently positive in the amygdala, thalamus, and basal ganglia. We also noted positive signal across several other brain regions, but no consistent signal across all subjects for these regions. This contrasts with AT8, which scored positive widely across the brain. This suggests that specific brain regions may be more predisposed to developing tau seeding in CTE despite widespread phospho-tau pathology.

Discussion

Chronic traumatic encephalopathy, described almost 100 years ago, is an emerging health concern. Its distinctive patterns of phospho-tau deposition and fibrillar tau morphologies mark it as a unique disorder [21]. Prior studies have identified tau seeding in extracts of CTE brain that transmit pathology to experimental animals, suggesting tau seeding underlies its progression [16, 37]. No systematic study of CTE has previously categorized the prevalence of tau seeding in relation to the phospho-tau pathology or examined seeding in relation to pathological progression.

The development of a simple cell-based assay to quantify pathological tau seeds in fixed brain tissues has created new opportunities to determine their prevalence and their relationship to classical measures of tau histopathology. In previous studies of AD and progressive age-related tauopathy, tau seeding in particular brain regions, including the transentorhinal/entorhinal cortex, superior temporal gyrus, and visual cortex was detected prior to phospho-tau pathology [11, 18], whereas in other areas, especially the locus coeruleus, phospho-tau pathology appeared before detectable tau seeding [18]. Hence, we tested the relationship of tau seeding to phospho-tau pathology across multiple brain regions and at various stages of CTE.

We quantified tau seeding in tissue samples from CTE cases and controls, comparing adjacent tissue sections for AT8 staining and counts of cells with phospho-tau pathology. We observed clear evidence of seeding in Stage III/IV CTE cases, although this was relatively restricted in its distribution compared to AT8 signal and cellular phospho-tau pathology. These findings are consistent with an observed shift toward more widespread phospho-tau pathology that occurs in Stage III/IV disease, whereas CTE Stage I/II cases are characterized by multifocal, largely cortical, pathology [1, 24]. We observed the strongest and most consistent seeding in the amygdala, basal ganglia and thalamus/subthalamic nucleus, with other regions showing more limited positivity in a subset of subjects. These findings are in line with the histopathological observations of increased thalamic, basal ganglia and amygdala phospho-tau pathology in stage III/IV disease [1, 24] as indicators of more severe disease [4]. Also, in Stage III/IV CTE, beginning around age 60 years, astrocytes that accumulate 4R phospho-tau in the CTE lesion increase in number [6]. There is a similar shift toward an increased neuronal 3R phospho-tau in Stage III/IV disease. Elucidating

the relationship between increased seeding and increases in astrocytic 4R and neuronal 3R phospho-tau in CTE are important subjects for future studies.

The findings in CTE contrast markedly with our prior studies of the distribution of seeding in AD, which clearly preceded the development of phospho-tau pathology in regions important for NFT staging [11, 18]. AD is an age-related tauopathy, whereas CTE is environmentally triggered, affects younger individuals, and worsens with age. A long latency divides cessation of head trauma and the development of clinical symptoms [15, 22]. Our findings in CTE suggest that the shift to progressive neurodegeneration in midlife might be associated with increased tau seeding in regions particularly vulnerable to these types of pathological tau assembly, or "strains."

We detected essentially no seeding in Stage I/II CTE. There are many possible explanations. First, the seeding assay itself may not have readily detected pathogenic forms of tau in CTE as efficiently as in our prior AD studies. This could be due to differences in embedding technique (polyethylene glycol (PEG) versus paraffin). Alternatively, the unique strain of tau assembly in CTE [16, 37], reflected in its fibril structure [9], may not seed as efficiently onto the P301S biosensors. Phospho-tau pathology in early CTE stages is limited to discrete foci, often in a perivascular distribution and within sulcal depths of the cortex [24]. Given paraffin samples were sectioned at 10 μm as compared to thicker PEG sections used in prior work [18], their relative fragility required a larger area of analysis. This may have diluted areas of limited pathology in these early stages, whereas our prior studies used PEG sections amenable to punch-biopsy sampling of highly specific sites of tau pathology [18]. Finally, phospho-tau signal in CTE may anticipate or over-represent the distribution of fibrillar tau pathology or seeding, reminiscent of our prior studies in AD in which phospho-tau signal within the LC at early NFT stages did not correlate with detectable seeding until later stages of the disease [18]. The LC is also involved in early stages of CTE [1], and no seeding was detected, although this finding is subject to the technical limitations described above.

In contrast to AD and other sporadic tauopathies, CTE is triggered by brain trauma, and the initial pathology (Stages I/II) is almost exclusively cortical. In this respect, it is remarkable that CTE seeding predominated in the amygdala, basal ganglia, and thalamus—brain regions involved in severe CTE, Stages III/IV. This suggests CTE-derived tau assemblies may be uniquely prone to amplify in these brain areas, and is consistent with our prior observations that tau strain identity governs regional brain vulnerability following inoculation into mice [16]. Cognitive impairment, behavior, mood and motor symptoms are common clinical features of severe (Stages III/IV) CTE [27]. It remains to be determined whether the clinical features of CTE reflect involvement of specific brain regions that are preferentially affected by specific tau aggregate conformation(s) generated from the initiating brain trauma. Future work that extends beyond these initial studies, including analysis of tau strains, their biochemical composition, and perhaps development of improved biosensors, could lead to a better understanding of the molecular origins of this devastating condition.

References

1. Alosco ML, Cherry JD, Huber BR, Tripodis Y, Baucom Z, Kowall NW et al. (2020) Characterizing tau deposition in chronic traumatic encephalopathy (CTE): utility of the McKee CTE staging scheme. Acta Neuropathol 140:495–512. 10.1007/s00401-020-02197-9 [PubMed: 32778942]

2. Alosco ML, Stein TD, Tripodis Y, Chua AS, Kowall NW, Huber BR et al. (2019) Association of white matter rarefaction, arteriolosclerosis, and tau with dementia in chronic traumatic encephalopathy. JAMA Neurol 76:1298–1308. 10.1001/jamaneurol.2019.2244 [PubMed: 31380975]

3. Armstrong RA, McKee AC, Stein TD, Alvarez VE, Cairns NJ (2017) A quantitative study of tau pathology in 11 cases of chronic traumatic encephalopathy. Neuropathol Appl Neurobiol 43:154–166. 10.1111/nan.12323 [PubMed: 26998921]

4. Bieniek KF, Cairns NJ, Crary JF, Dickson DW, Folkerth RD, Keene CD et al. (2021) The second NINDS/NIBIB consensus meeting to define neuropathological criteria for the diagnosis of chronic traumatic encephalopathy. J Neuropathol Exp Neurol 80:210–219. 10.1093/jnen/nlab001 [PubMed: 33611507]

5. Braak H, Braak E (1991) Neuropathological stageing of Alzheimer-related changes. Acta Neuropathol 82:239–259. 10.1007/BF00308809 [PubMed: 1759558]

6. Cherry JD, Kim SH, Stein TD, Pothast MJ, Nicks R, Meng G et al. (2020) Evolution of neuronal and glial tau isoforms in chronic traumatic encephalopathy. Brain Pathol 30:913–925. 10.1111/bpa.12867 [PubMed: 32500646]

7. Cherry JD, Tripodis Y, Alvarez VE, Huber B, Kiernan PT, Daneshvar DH et al. (2016) Microglial neuroinflammation contributes to tau accumulation in chronic traumatic encephalopathy. Acta Neuropathol Commun 4:112. 10.1186/s40478-016-0382-8 [PubMed: 27793189]

8. DeVos SL, Corjuc BT, Oakley DH, Nobuhara CK, Bannon RN, Chase A et al. (2018) Synaptic tau seeding precedes tau pathology in human Alzheimer's disease brain. Front Neurosci. 10.3389/fnins.2018.00267

9. Falcon B, Zivanov J, Zhang W, Murzin AG, Garringer HJ, Vidal R et al. (2019) Novel tau filament fold in chronic traumatic encephalopathy encloses hydrophobic molecules. Nature 568:420–423 [PubMed: 30894745]

10. Furman JL, Holmes BB, Diamond MI (2015) Sensitive detection of proteopathic seeding activity with FRET flow cytometry. J Vis Exp. 10.3791/53205

11. Furman JL, Vaquer-Alicea J, White CL, Cairns NJ, Nelson PT, Diamond MI (2017) Widespread tau seeding activity at early Braak stages. Acta Neuropathol 133:91–100. 10.1007/s00401-016-1644-z [PubMed: 27878366]

12. Geddes JF, Vowles GH, Nicoll JA, Révész T (1999) Neuronal cytoskeletal changes are an early consequence of repetitive head injury. Acta Neuropathol 98:171–178. 10.1007/s004010051066 [PubMed: 10442557]

13. Goldstein LE, Fisher AM, Tagge CA, Zhang XL, Velisek L, Sullivan JA et al. (2012) Chronic traumatic encephalopathy in blast-exposed military veterans and a blast neurotrauma mouse model. Sci Transl Med. 10.1126/scitranslmed.3003716

14. Holmes BB, Furman JL, Mahan TE, Yamasaki TR, Mirbaha H, Eades WC et al. (2014) Proteopathic tau seeding predicts tauopathy in vivo. Proc Natl Acad Sci USA 111:E4376–E4385. 10.1073/pnas.1411649111 [PubMed: 25261551]

15. Katz DI, Bernick C, Dodick DW, Mez J, Mariani ML, Adler CH et al. (2021) National institute of neurological disorders and stroke consensus diagnostic criteria for traumatic encephalopathy syndrome. Neurology 96:848–863. 10.1212/wnl.0000000000011850 [PubMed: 33722990]

16. Kaufman SK, Sanders DW, Thomas TL, Ruchinskas AJ, Vaquer-Alicea J, Sharma AM et al. (2016) Tau prion strains dictate patterns of cell pathology, progression rate, and regional vulnerability in vivo. Neuron 92:796–812. 10.1016/j.neuron.2016.09.055 [PubMed: 27974162]

17. Kaufman SK, Thomas TL, Del Tredici K, Braak H, Diamond MI (2017) Characterization of tau prion seeding activity and strains from formaldehyde-fixed tissue. Acta Neuropathol Commun 5:41. 10.1186/s40478-017-0442-8 [PubMed: 28587664]

18. Kaufman SK, Del Tredici K, Thomas TL, Braak H, Diamond MI (2018) Tau seeding activity begins in the transentorhinal/entorhinal regions and anticipates phospho-tau pathology in Alzheimer's disease and PART. Acta Neuropathol 136:57–67. 10.1007/s00401-018-1855-6 [PubMed: 29752551]

19. Lee VM-Y, Goedert M, Trojanowski JQ (2001) Neurodegenerative tauopathies. Annu Rev Neurosci 24:1121–1159. 10.1146/annurev.neuro.24.1.1121 [PubMed: 11520930]

20. Martland HS (1928) Punch drunk. J Am Med Assoc 91:1103–1107. 10.1001/jama.1928.02700150029009

21. McKee AC, Cairns NJ, Dickson DW, Folkerth RD, Dirk Keene C, Litvan I et al. (2016) The first NINDS/NIBIB consensus meeting to define neuropathological criteria for the diagnosis of chronic traumatic encephalopathy. Acta Neuropathol 131:75–86. 10.1007/s00401-015-1515-z [PubMed: 26667418]

22. McKee AC, Cantu RC, Nowinski CJ, Hedley-Whyte ET, Gavett BE, Budson AE et al. (2009) Chronic traumatic encephalopathy in athletes: progressive tauopathy after repetitive head injury. J Neuropathol Exp Neurol 68:709–735 [PubMed: 19535999]

23. McKee AC, Daneshvar DH, Alvarez VE, Stein TD (2014) The neuropathology of sport. Acta Neuropathol 127:29–51 [PubMed: 24366527]

24. McKee AC, Stein TD, Nowinski CJ, Stern RA, Daneshvar DH, Alvarez VE et al. (2013) The spectrum of disease in chronic traumatic encephalopathy. Brain 136:43–64. 10.1093/brain/aws307 [PubMed: 23208308]

25. McKhann G, Drachman D, Folstein M, Katzman R, Price D, Stadlan EM (1984) Clinical diagnosis of Alzheimer's disease: Report of the NINCDS-ADRDA work group under the auspices of Department of Health and Human Services Task Force on Alzheimer's Disease. Neurology 34:939–944. 10.1212/wnl.34.7.939 [PubMed: 6610841]

26. McKhann GGM, Knopman DS, Chertkow H, Hyman BT, Jack CRJ, Kawas CH et al. (2012) The diagnosis of dementia due to Alzheimer's disease: recommendations from the National Institute on Aging-Alzheimer's Association workgroups on diagnostic guidelines for Alzheimer's disease. Alzheimers Dement 7:263–269. 10.1016/j.jalz.2011.03.005.The

27. Mez J, Daneshvar DH, Kiernan PT, Abdolmohammadi B, Alvarez VE, Huber BR et al. (2017) Clinicopathological evaluation of chronic traumatic encephalopathy in players of American football. J Am Med Assoc 318:360–370. 10.1001/jama.2017.8334

28. Mez J, Solomon TM, Daneshvar DH, Murphy L, Kiernan PT, Montenigro PH et al. (2015) Assessing clinicopathological correlation in chronic traumatic encephalopathy: rationale and methods for the UNITE study. Alzheimer's Res Ther 7:1–14. 10.1186/s13195-015-0148-8 [PubMed: 26584966]

29. Mirbaha H, Chen D, Morazova OA, Ruff KM, Sharma AM, Liu X et al. (2018) Inert and seed-competent tau monomers suggest structural origins of aggregation. Elife. 10.7554/eLife.36584

30. Mirbaha H, Holmes BB, Sanders DW, Bieschke J, Diamond MI (2015) Tau trimers are the minimal propagation unit spontaneously internalized to seed intracellular aggregation. J Biol Chem 290:14893–14903. 10.1074/jbc.M115.652693 [PubMed: 25887395]

31. Montine TJ, Phelps CH, Beach TG, Bigio EH, Cairns NJ, Dickson DW et al. (2012) National institute on aging-Alzheimer's association guidelines for the neuropathologic assessment of Alzheimer's disease: a practical approach. Acta Neuropathol 123:1–11. 10.1007/s00401-011-0910-3 [PubMed: 22101365]

32. Nelson PT, Dickson DW, Trojanowski JQ, Jack CR, Boyle PA, Arfanakis K et al. (2019) Limbic-predominant age-related TDP-43 encephalopathy (LATE): consensus working group report. Brain 142:1503–1527. 10.1093/brain/awz099 [PubMed: 31039256]

33. Omalu BI, DeKosky ST, Minster RL, Kamboh MI, Hamilton RL, Wecht CH (2005) Chronic traumatic encephalopathy in a National Football League player. Neurosurgery 57:128–133. 10.1227/01.NEU.0000163407.92769.ED

34. Sanders DW, Kaufman SK, DeVos SL, Sharma AM, Mirbaha H, Li A et al. (2014) Distinct tau prion strains propagate in cells and mice and define different tauopathies. Neuron. 10.1016/j.neuron.2014.04.047

35. Sanders DW, Kaufman SK, Holmes BB, Diamond MI (2016) Prions and protein assemblies that convey biological information in health and disease. Neuron. 10.1016/j.neuron.2016.01.026

36. Seeley WW, Crawford RK, Zhou J, Miller BL, Greicius MD (2009) Neurodegenerative diseases target large-scale human brain networks. Neuron 62:42–52. 10.1016/j.neuron.2009.03.024 [PubMed: 19376066]

37. Woerman AL, Aoyagi A, Patel S, Kazmi SA, Lobach I, Grinberg LT et al. (2016) Tau prions from Alzheimer's disease and chronic traumatic encephalopathy patients propagate in cultured cells. Proc Natl Acad Sci USA 113:E8187–E8196. 10.1073/pnas.1616344113 [PubMed: 27911827]
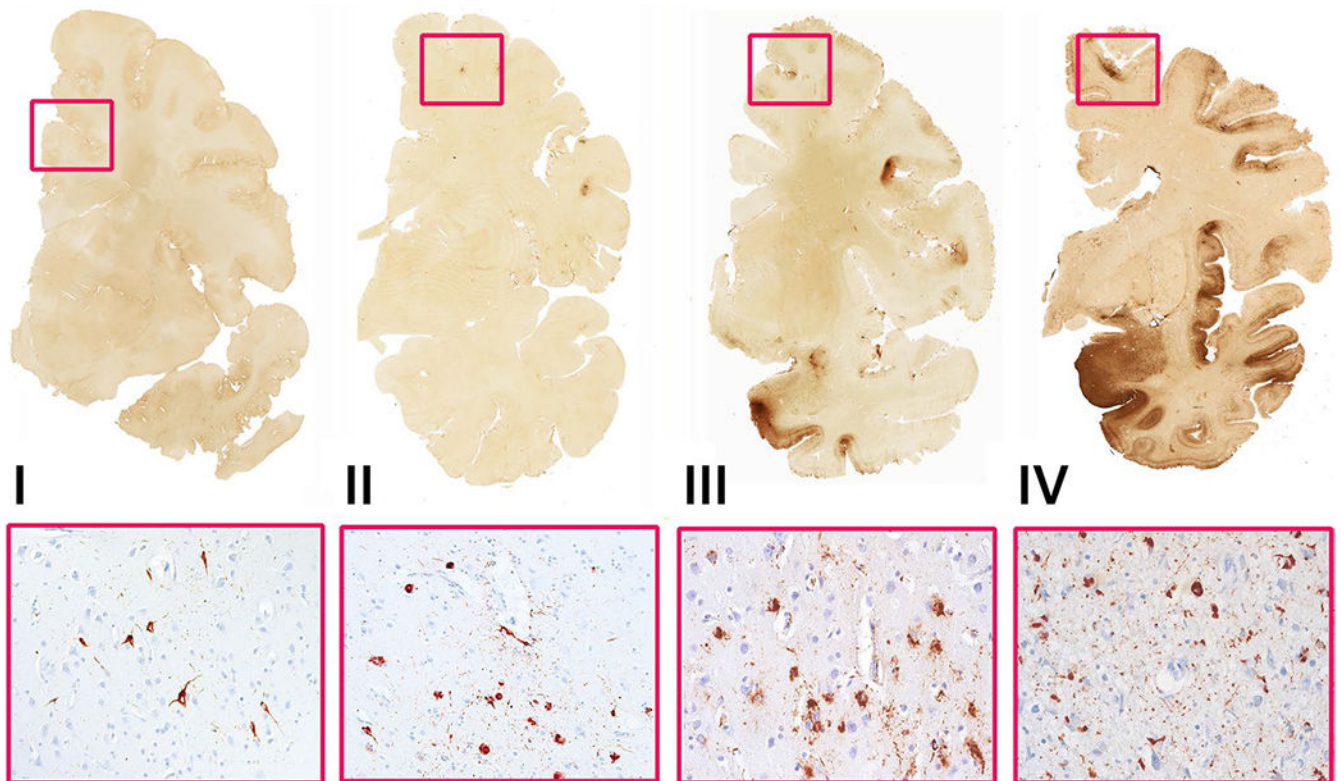
Fig. 1.

Pathology of CTE, examples from the CTE cohort. 50 μm free-floating coronal sections were stained with mouse monoclonal antibody (AT8; Pierce Endogen) for phosphorylated tau (p-tau). For all microscopic images, 10 μm paraffin-embedded tissue sections were stained with AT8. Positive p-tau staining appears dark red, hematoxylin counterstain. Magnification is ×400. Stage I: Case 6. 23-Year-old NFL player with isolated CTE lesion in frontal cortex (red rectangle, top); corresponding perivascular CTE p-tau lesion at the depths of the superior frontal sulcus (red rectangle, bottom). Stage II: Case 13. 25-Year-old former college football player with 3 CTE lesions in frontal cortex (red rectangle, top); corresponding perivascular CTE p-tau lesion at depth of the sulcus in dorsolateral frontal cortex (red rectangle, bottom). Stage III: Case 19. 50-Year-old former NFL player with multiple, large confluent CTE lesions in the frontal, parietal and temporal cortices and diffuse neurofibrillary degeneration of entorhinal cortex and amygdala (red rectangle, top); corresponding perivascular CTE p-tau lesion at depths of the sulcus in dorsolateral frontal cortex (red rectangle, bottom). Stage IV: Case 31. 68-Year-old former NFL player with large confluent CTE lesions involving most of the frontal, insular and temporal cortex, there is severe diffuse p-tau deposition in the amygdala and entorhinal cortex (red rectangle, top); corresponding perivascular CTE p-tau lesion at depths of the sulcus in dorsolateral frontal cortex (red rectangle, bottom)
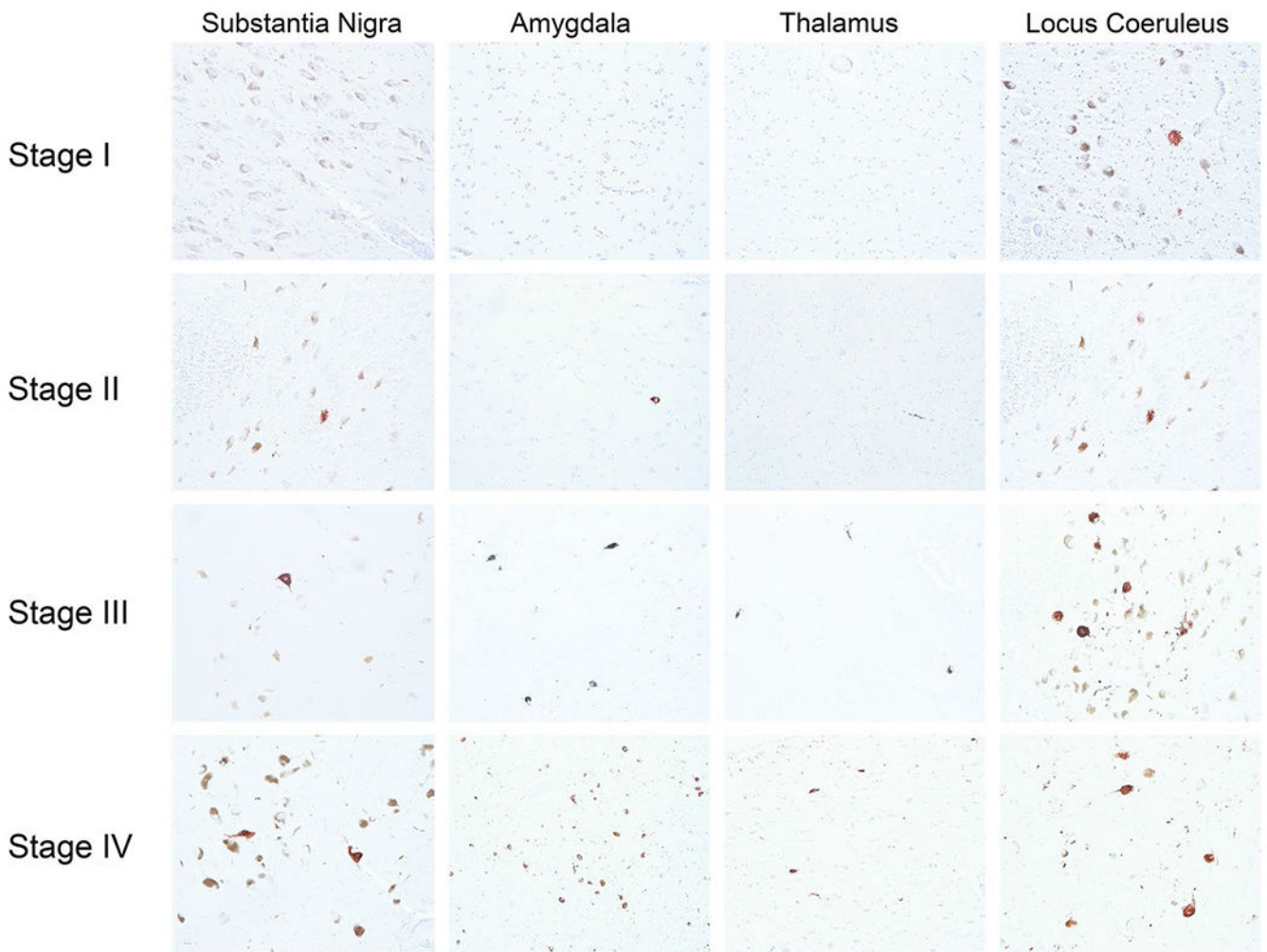
Fig. 2.
Regional density of AT8 immunoreactive neurofibrillary tangles in CTE stages I–IV. Anti-p-tau antibody (AT8) was used to stain multiple CTE brain regions at different disease stages. In stage I, in addition to isolated perivascular CTE lesions in the cortex, there are sparse neurofibrillary tangles (NFTs) in locus coeruleus but no NFTs in substantia nigra, amygdala or thalamus (case 6). In stage II, in addition to perivascular CTE lesions in the cortex, sparse NFTs are found in the substantia nigra and locus coeruleus (case 12). In stage III CTE, moderate NFTs are found in the substantia nigra, locus coeruleus, amygdala and thalamus (case 19). In stage IV CTE, frequent NFTs are found in the substantia nigra, locus coeruleus, amygdala and thalamus (case 32). All images are ×200 magnification
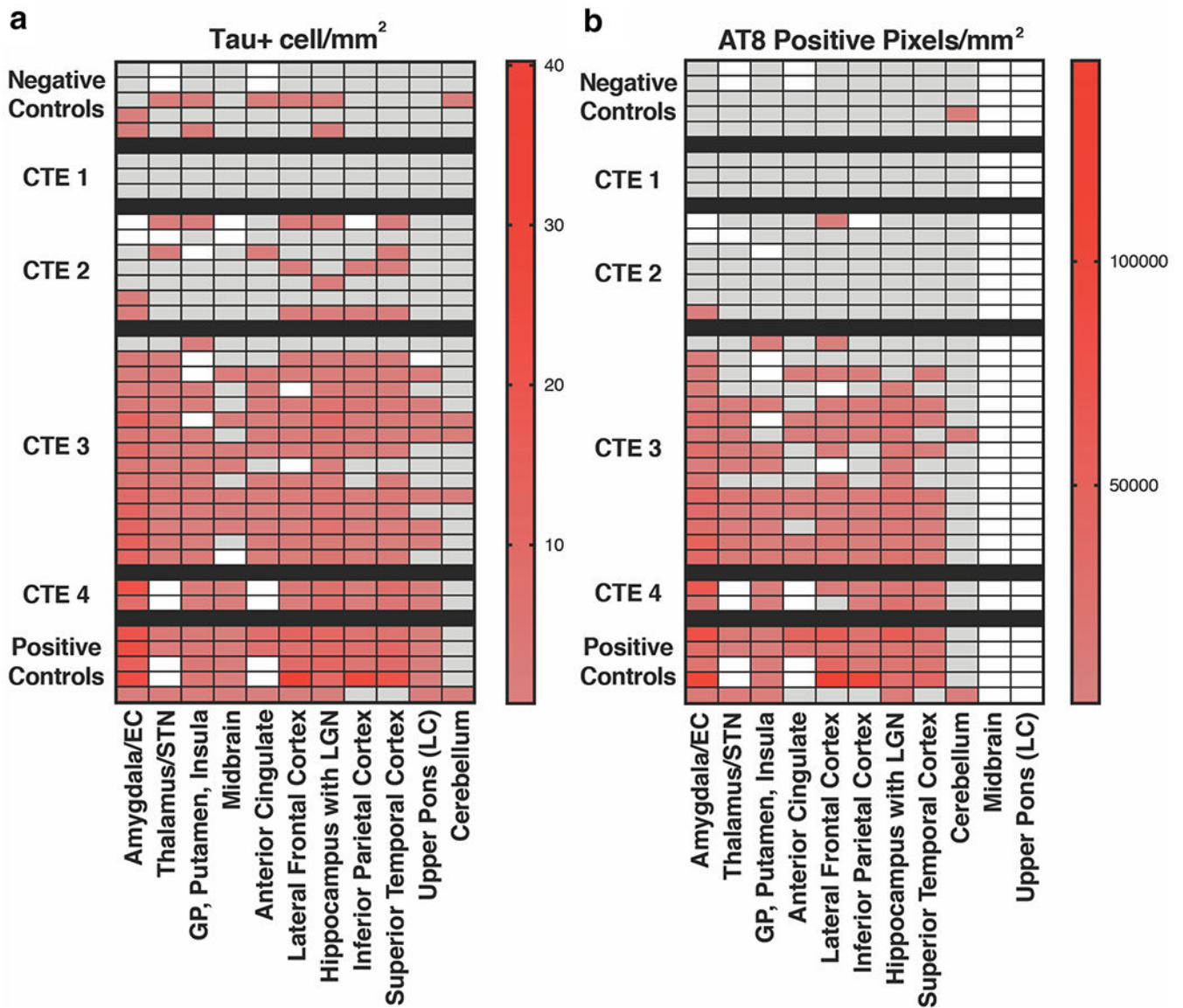
Fig. 3.

Quantification of tau AT8 histopathology in CTE. **a** p-tau pathology was quantified in specified tissue blocks by immunostain (AT8). Whole sections were outlined to determine total area of interest. White squares denote brain regions that were not available for analysis. Tau positive cells/mm^2 is displayed using a 5 SD cutoff above control samples and quantified on a linear scale in arbitrary units. Gray delineates samples that were below this threshold. **b** Total AT8 positive pixels/mm^2 were quantified in specified tissue blocks using image analysis and automated counting software as previously described [7]. Positive samples are displayed with a 5 SD cutoff above control samples, and quantified on a linear scale. Tissue blocks were selected based on previous work identifying brain regions of interest in CTE [24]. Midbrain and pons data could not be included in an automated assessment of AT8 histopathology due to neuromelanin pigmentation present in the substantia nigra and locus coeruleus, respectively

Seeding Activity
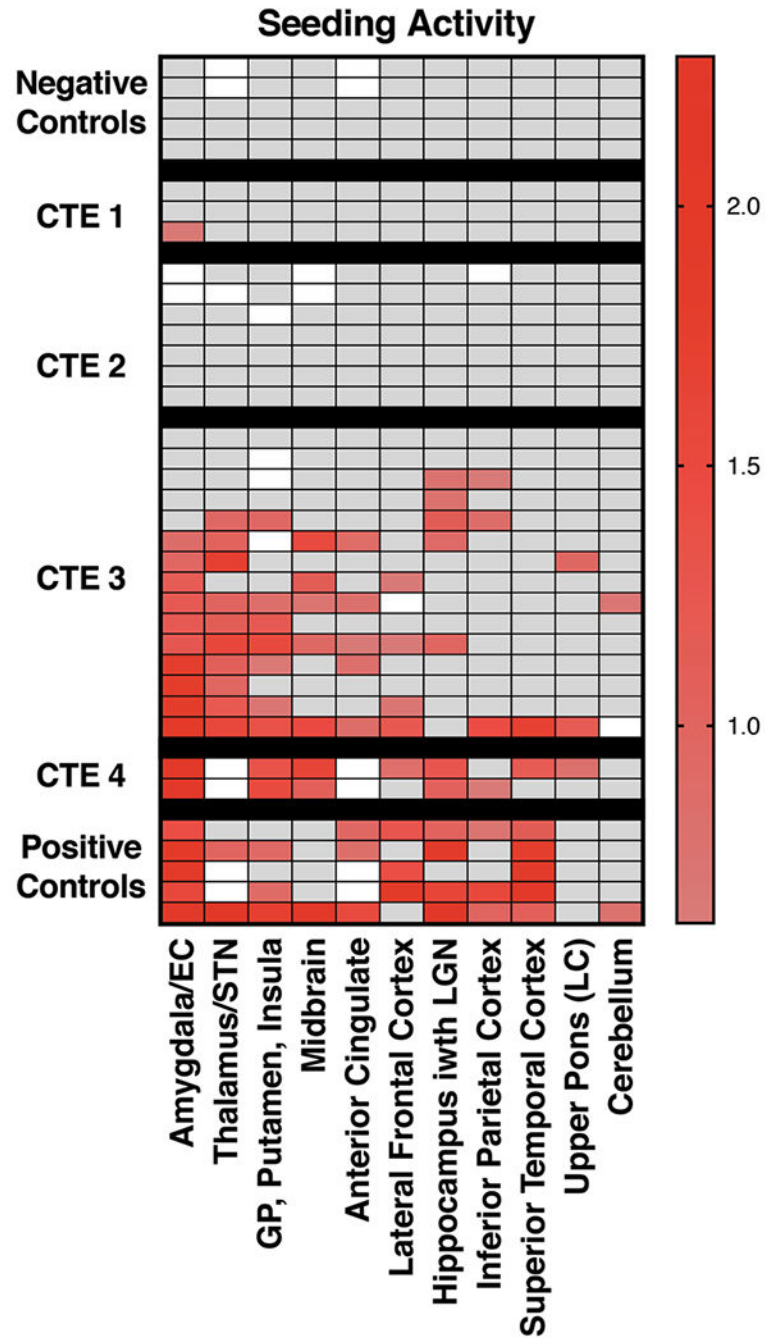
Fig. 4.
Tau seeding is readily detected at CTE stages III/IV especially in limbic structures. Tau seeding was quantified in a blinded fashion across CTE subjects, positive controls from AD and FTD subjects, and negative control subjects. Tissue was homogenized and transduced into biosensor cells. Tau seeding was quantified using flow cytometry as the percentage of FRET-positive cells × median fluorescence intensity and normalized to negative control sample seeding. Positive signal is displayed using a 5 SD cutoff above negative control

samples, and quantified using a logarithmic scale. White squares denote brain regions that were not available for analysis. Gray delineates samples that were below this threshold

Table 1

Characteristics of study subjects

	Age	G	Race	Sport	Level of play	Cause of death	Diagnosis	AD	Aß	as	TDP	Vas	Dementia Y/N	PMI
1	61	M	White	n/a	n/a	Cardiac	Control	0	+	0	0	0	No	24
2	21	M	White	n/a	n/a	Suicide	Control	0	0	0	0	0	No	15
3	63	M	White	n/a	n/a	Cancer	Control	0	0	0	0	0	No	48
4	57	M	White	n/a	n/a	Cancer	Control	0	0	0	0	0	No	24
5	69	F	White	n/a	n/a	Unknown	Control	0	0	0	0	0	No	69
6	23	M	Black	Football	Professional	Suicide	CTE I	0	0	0	0	0	No	unk
7	24	M	White	Soccer	College	Suicide	CTE I	0	0	0	0	0	No	36
8	24	M	White	Football	HS	MVA	CTE I	0	0	0	0	0	No	48
9	25	M	White	Football	HS	Suicide	CTE II	0	0	0	0	0	No	24
10	25	M	Black	Football	Professional	Suicide	CTE II	0	0	0	0	0	No	76
11	30	M	White	Football	Professional	Overdose	CTE II	0	0	0	0	0	No	unk
12	26	M	White	Football	College	Suicide	CTE II	0	0	0	0	0	No	unk
13	28	M	White	Hockey	Professional	Overdose	CTE II	0	0	0	0	0	No	24
14	32	M	White	Football	College	Suicide	CTE II	0	0	0	0	0	No	unk
15	25	M	White	Football	College	Infection	CTE II	0	0	0	0	0	No	2
16	62	M	White	Football	Professional	Cardiac	CTE III	0	+	0	0	+	Yes	72
17	49	M	Black	Football	Professional	Cardiac	CTE III	0	0	0	0	0	No	48
18	46	M	White	Football	Professional	Cardiac	CTE III	0	+	0	0	0	No	72
19	50	M	Black	Football	Professional	Suicide	CTE III	0	0	0	+	0	No	24
20	52	M	White	Football	Professional	Encephalopathy	CTE III	0	0	0	0	0	Yes	24
21	56	M	Black	Football	Professional	Cardiac	CTE III	0	0	0	0	0	No	10
22	60	M	Black	Football	Professional	Cardiac	CTE III	0	0	0	0	0	No	unk
23	72	M	White	Football	Professional	Cancer	CTE III	0	0	0	+	+	No	24
24	58	M	White	Football	Professional	Cardiac	CTE III	0	0	0	0	0	No	24
25	71	M	White	Football	Professional	Cancer	CTE III	0	0	0	0	0	No	unk
26	61	M	White	Boxing	Professional	Liver disease	CTE III	0	0	0	+	0	No	unk
27	76	M	Black	Football	Professional	Cardiac	CTE III	0	+	0	+	0	Yes	57
28	67	M	White	Football	Professional	Cardiac	CTE III	0	+	0	+	0	No	unk

	Age	G	Race	Sport	Level of play	Cause of death	Diagnosis	AD	Aβ	as	TDP	Vas	Dementia Y/N	PMI
29	69	M	White	Football	Professional	Cancer	CTE III	0	0	0	+	0	No	36
30	78	M	White	Football	Professional	Suicide	CTE III	0	++	0	+	0	No	unk
31	68	M	White	Football	Professional	Cancer	CTE IV	0	+	0	+	0	No	3
32	66	M	White	Football	Professional	Cardiac	CTE IV	0	+	0	0	0	Yes	24
33	74	M	White	n/a	n/a	FTT	AD Braak VI	AD	+++	0	0	0	Yes	9
34	72	M	White	n/a	n/a	FTT	AD Braak VI	AD	+++	0	0	0	Yes	17
35	67	M	White	n/a	n/a	FTT	AD Braak V	AD	+++	0	0	0	Yes	12
36	57	F	White	n/a	n/a	FTT	AD Braak V	AD	+++	0	0	0	Yes	17
37	80	F	White	n/a	n/a	Cancer	FTLD-tau	0	0	++	0	+++	Yes	7

n/a not applicable, *HS* high school, *FTT* failure to thrive, *AD* Alzheimer's disease, *Aβ* beta-amyloid diffuse plaques, *as* alpha-synuclein, *TDP* transactive response DNA binding protein of 43 kDa (TDP-43), *Vas* vascular disease, *PMI* post-mortem interval (hours), *FTLD-tau* frontotemporal lobar degeneration-tau, *CTE* chronic traumatic encephalopathy